

A Compact Realization of Composite Low-pass Filter for Monolithic Microwave Integrated Circuit Applications

Navid Arbabi,¹ Mohammad Almalkawi,² Vijay Devabhaktuni,² Mustapha Yagoub,³ Arjuna Madanayake⁴

¹ Department of ECE, Concordia University, Montreal, QC, Canada

² Department of EECS, The University of Toledo, Toledo, OH 43606

³ School of Information Technology and Engineering, University of Ottawa, Ottawa, ON, Canada

⁴ Department of ECE, The University of Akron, Akron, OH 44325

Received 5 May 2011; accepted 12 July 2011

ABSTRACT: A compact realization of composite low-pass filter is presented in this article. The filter is realized using on-chip spiral inductors and metal–insulator–metal capacitors and features an attenuation pole near the cutoff frequency leading to a sharper attenuation response. As well, it offers good matching properties in the passband. Space-mapping-based algorithm is used in the design/optimization of spiral inductors toward achieving high quality factors at the filter cutoff frequency. The realization of the proposed filter is compact in size, suitable for monolithic microwave integrated circuit applications, and exhibit broad upper stopband frequency characteristics. © 2011 Wiley Periodicals, Inc. *Int J RF and Microwave CAE* 22:147–152, 2012.

Keywords: composite low-pass filter; MIM capacitor; space-mapping; spiral inductor

I. INTRODUCTION

Microwave low-pass filters (LPFs) are essential components for a plethora of applications such as radio frequency (RF) test equipments, wireless communications, radar, microwave imaging, and remote sensing. Modern systems impose stringent requirements on filters such as small size, low insertion loss, and high selectivity. A particularly attractive approach to the design of microwave LPFs that satisfy such stringent requirements and specifications uses composite LPF design [1]. A basic composite LPF consists of identical sections in cascade to form a ladder configuration, where the sections are designed using the image method; here, the number of sections in the ladder network determines the stop band rejection of the filter. It is recalled that such image filters are characterized by their image impedance which is defined as the characteristic impedance of an infinite length transmission line made up identical ladder sections [2]. Recently, a

composite LPF having cutoff frequency at 1.5 GHz, and based on microstrip lines, has been described in Ref. 3. This filter suffers from ripples in the passband and occupies large amount of chip area. Further, there is potential for increasing the slope of the transition band as it moves toward the stopband of the filter.

The objective in this article is to realize the well-known composite LPF approach with a desired cutoff frequency using on-chip spiral inductors and metal–insulator–metal (MIM) capacitors suitable for MMIC technology. Here, a recently proposed computer-aided design algorithm [4] based on the method of space-mapping is exploited to rapidly yet accurately optimize on-chip spiral inductors exhibiting high quality factors (Q_s) at the desired cutoff frequency. Compared to previously reported composite LPFs [3, 5], the proposed realization is compact ($1.4 \times 0.8 \text{ mm}^2$), exhibits sharper cutoff response with a better rejection band, and has a flat passband with a relatively low insertion loss.

The article is organized as follows. Section II discusses design aspects of composite LPFs. Section III deals with its practical realization and simulated results. Finally, conclusions are given in Section IV.

Correspondence to: V. Devabhaktuni; e-mail: Vijay.Devabhaktuni@utoledo.edu

DOI 10.1002/mmce.20566

Published online 4 November 2011 in Wiley Online Library (wileyonlinelibrary.com).

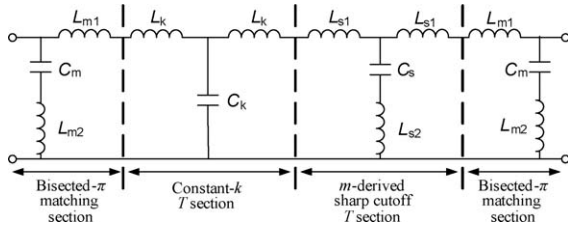


Figure 1 Schematic of a composite LPF.

II. SYNTHESIS OF COMPOSITE LPF

Design of LPFs, which are compact and exhibit sharper attenuation responses, is challenging. Traditional approaches (e.g., Butterworth, Chebyshev, and Elliptic) entail higher-order topologies to achieve a flat passband and sharp attenuation [6, 7] and hence directly contradict the design requirements. A composite LPF can be promising in such challenging scenarios. A composite LPF consists of four sections, namely, a constant- k , an m -derived sharp cutoff, and two m -derived matching sections [1, 2, 8]. Schematic of a composite LPF is depicted in Figure 1. The constant- k section by itself can be used to design either a low-pass or a high-pass filter. However, such filters have two drawbacks. The signal attenuation rate after the cutoff point is not very sharp, and the image impedance is not constant with frequency. We propose that to overcome these drawbacks, m -derived filter sections (a sharp cutoff T section and two matching π sections) are added. We also propose that the aforementioned sections are designed using the image parameter method. The image parameter method is useful for the design of simple filters and provides a link between infinite periodic structure and practical filter design [9].

In the following design example, the cutoff frequency have been arbitrary selected at $f_c = 2.8$ GHz. The proposed design starts with the calculation of constant- k and m -derived T sections, which take into account the desired characteristic impedance R_0 and a parameter m of the T section (which sets the placement of an attenuation pole near f_c). In the proposed design procedure, different values of $m < 0.6$ for the T section are evaluated, leading to the final choice of $m = 0.3$ resulting in a frequency response that meets design specifications. Next, the matching π sec-

TABLE I Theoretical Expressions and Values of the Lumped Elements

Sections	Lumped Elements	Expressions	Values
Constant- k T section	L	$2R_0/(2\pi f_c)$	5.684 nH
	C	$2/(R_0 2\pi f_c)$	2.274 pF
m -Derived sharp cutoff ($m = 0.3$) T section	L_k	$L/2$	2.842 nH
	C_k	C	2.274 pF
m -Derived matching ($m = 0.6$) bisectioned- π section	L_{s1}	$mL/2$	0.853 nH
	L_{s2}	$L(1 - m^2)/(4m)$	4.310 nH
	C_s	mC	0.682 pF
	L_{m1}	$mL/2$	1.705 nH
	L_{m2}	$L(1 - m^2)/(2m)$	3.031 nH
	C_m	$mC/2$	0.682 pF

$f_c = 2.8$ GHz and $R_0 = 50 \Omega$.

tions are designed, with their corresponding parameter m set to 0.6 for minimizing the image impedance variation with frequency at the input and output ports. The sections are cascaded to realize a LPF of lower order and smaller size. Such a filter results in a steeper attenuation rate in the transition band (i.e., after the cutoff frequency). The pole can be flexibly adjusted by changing m . Expressions as well as the values of the lumped elements are summarized in Table I. Figure 2 shows the composite LPF design obtained after combining series pairs of inductors and optimizing the lumped element values using Agilent Advanced Design System (ADS) [10].

III. COMPACT REALIZATION USING SPIRAL INDUCTORS AND MIM CAPACITOR

The next step is to realize the filter schematic in Figure 2, in particular, the inductors and the capacitors. Here, we use rectangular spiral inductors and MIM capacitors toward realizing a compact composite LPF. Spiral inductors and MIM capacitors possess relatively lower Q s compared to their distributed counterparts owing to both smaller dimensions and multilevel fabrication processes. To their advantage, on-chip spiral inductors and MIM capacitors are lower cost and have wider bandwidths [11]. The following steps describe the proposed composite LPF realization.

A. Choice of Substrate and Metal Layers

A 300- μm silicon substrate with a dielectric constant of 11.9 and a loss tangent of 0.005 [12], and a 5- μm silicon dioxide with a dielectric constant of 4 and a loss tangent of 0.001, are used as the substrate and the oxide layers, respectively. Two copper metal layers M_1 and M_2 of 1 μm thickness and 5.8×10^7 S/m conductivity are used for the spiral inductor and the underpass, respectively. These metal layers are also used for the MIM capacitor plates. The cross sections and top views of spiral inductors and MIM capacitors are depicted in Figures 3 and 4, respectively.

B. Optimization of spiral Inductors and MIM Capacitors

The objective of this step is to separately realize each of the six inductors and four capacitors with specific values at 2.8 GHz as indicated in Figure 2. Note, at GHz frequencies, eddy currents and self-resonance inside the spiral inductor affects the inductor's performance in terms of both its inductance and Q [13]. As such, accurate design of inductors considering such phenomena demands the use of CPU-expensive electromagnetic (EM) simulations. Our recent space-mapping-based algorithm, which exploits the sequential quadratic programming (SQP) technique for coarse

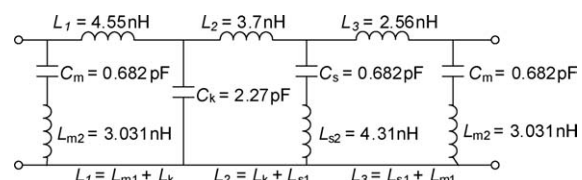


Figure 2 Lumped equivalent circuit prototype of the composite LPF.

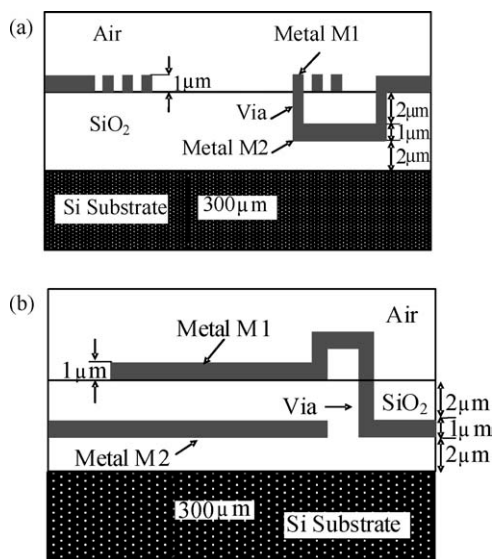


Figure 3 Cross section of (a) spiral inductor and (b) MIM capacitor.

model optimization is applied for the design/optimization of all six inductors of Figure 2 [4]. Starting with desired frequency range and inductance, the algorithm leads to spiral inductor designs with high Q_s , using minimal amounts of EM data. Considering one inductor at a time, the algorithm first improves the inductor's circuit model, until the circuit model response matches with the EM-simulated response of Zeland IE3D [14]. This is accomplished by iteratively adjusting the preassigned parameters [4].

The next step is to optimize the resulting improved circuit model leading to the specified inductance value at 2.8 GHz. This is achieved by iteratively adjusting the spiral inductor geometry (as the circuit model parameters relate to the inductor geometry). The algorithm leads to a spiral inductor layout offering the desired inductance and an

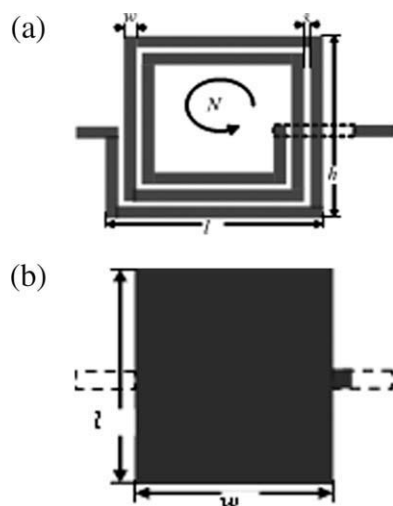


Figure 4 Top view of (a) spiral inductor and (b) MIM capacitor.

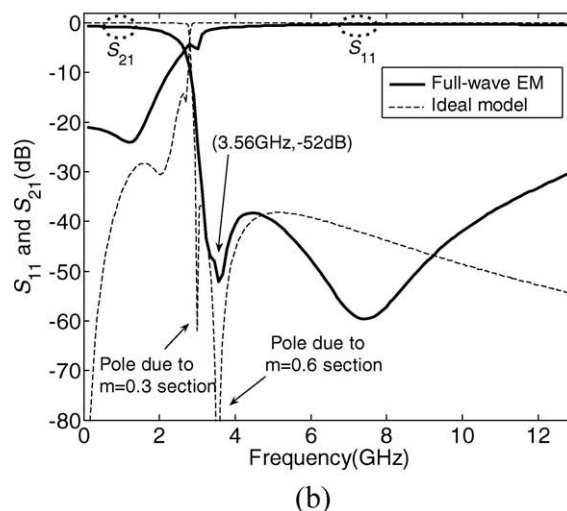
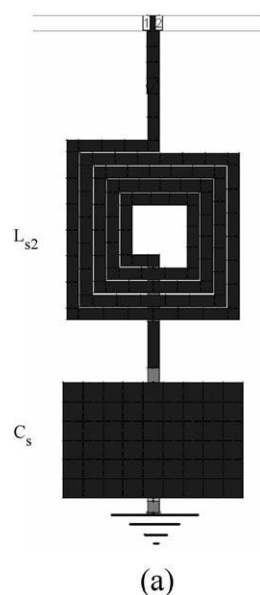


Figure 5 (a) A series LC resonator and (b) its frequency characteristics using EM simulations.

optimal Q . In this work, Q_s of all six spiral inductors are in the [7, 9] range. It is ensured that the self-resonance frequency of each inductor is much higher than 2.8 GHz.

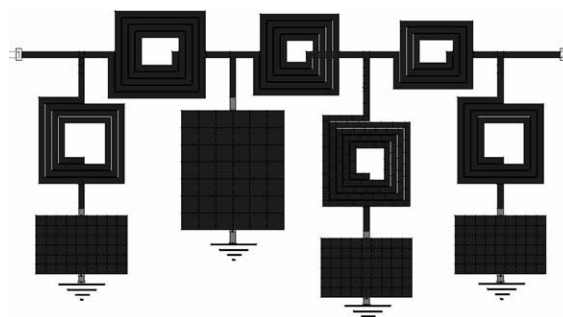


Figure 6 Layout of the proposed composite LPPF in Zeland IE3D.

TABLE II Dimensions of Spiral Inductors in the Proposed Composite LPF

Inductors	l (μm)	h (μm)	w (μm)	s (μm)	N
L_1	244	220	15	2	4.5
L_2	215	204	15	2	4.5
L_3	200	172	15	2	3.5
L_{m2}	219	216	15	2	3.5
L_{s2}	231	220	15	2	4.5

The four MIM capacitors are initially designed using semianalytical equations [11], and the initial designs are optimized in Zeland IE3D leading to specified capacitances at 2.8 GHz. To connect all these elements, extra transmission lines are needed in the shunt arms of the circuit. These lines affect the inductance and capacitance values. As such, the dimensions of inductors/capacitors had to be fine-tuned to account for the extra lines.

C. Optimization of Resonators

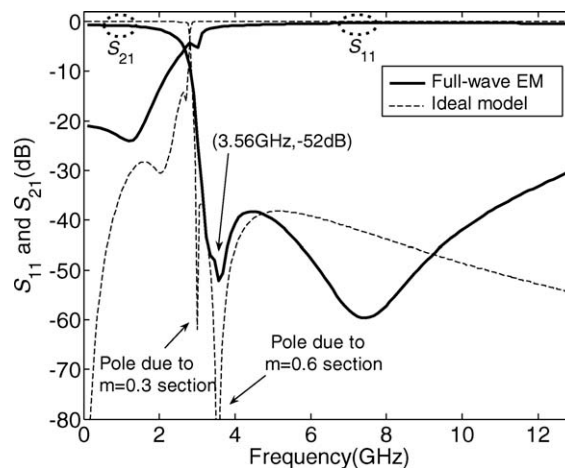
Series inductor-capacitor (LC) resonators in the shunt arms of the filter require additional fine-tuning by EM simulations to ensure operation at the desired resonant frequencies. For instance, Figure 5(a) shows one of the three LC resonators representing L_{s2} and C_s of Figure 2, which is expected to provide the first pole of the composite LPF at 3 GHz. Figure 5(b) shows resonance of the LC resonator at 2.99 GHz using Zeland IE3D simulations.

IV. RESULTS AND DISCUSSIONS

Finally, all the aforementioned sections are combined to build the complete composite LPF, whose layout is shown in Figure 6. Physical dimensions of inductors/capacitors in the final LPF are tabulated in Tables II and III, respectively. For comparison, ideal ADS simulations and actual Zeland IE3D simulations are presented in Figure 7. EM simulations show a flat response with no ripple, good matching properties, rejection of the attenuated pole as high as 59.5 dB, and low insertion loss in the passband (0.76 dB at 0.19 GHz). The cutoff frequency is 2.6 GHz, and the stopband attenuation is greater than 20 dB over a 12 GHz bandwidth. The slope of S_{21} between cutoff frequency and the first pole is 50 dB/GHz, which is much higher than the 25 dB/GHz slope of the LPF reported in [3]. As well, the proposed filter occupies a compact area of $1.4 \times 0.8 \text{ mm}^2$, which is much smaller than $67 \times 23 \text{ mm}^2$ occupied by the LPF in [3, 5]. As seen in Table IV, there is a reasonable agreement between the performance of the proposed filter and that of its ideal counterpart. Minor discrepancies are due to both parasitic effects and

TABLE III Dimensions of MIM Capacitors in the Proposed Composite LPF

Capacitors	l (μm)	w (μm)
C_m	230	148
C_k	258	300
C_s	230	150

**Figure 7** S -Parameter responses of the composite LPF obtained from EM simulations and ideal model simulations using Agilent ADS.**TABLE IV** Comparison of the Performances of the Proposed Filter Obtained Using Ideal Model and Full-Wave Simulations

	Loss at 0.19 GHz (dB)	f_c (GHz)	f of First Pole (GHz)	Attenuation of First Pole (dB)
Ideal model simulations	0	2.8	3	62
Full-wave EM simulations	0.76	2.6	3.56	52

losses of the spiral inductors and MIM capacitors, which are not considered by the ideal model.

V. CONCLUSIONS

A composite LPF based on spiral inductors and MIM capacitors for MMIC applications was presented. The realization of the proposed filter with finite frequency transmission zeros that are closely positioned to the passband offers a sharp cutoff response. A flat passband with minimal insertion loss levels and wide rejection band performance is achieved. The overall size of the filter is considerably reduced compared to other filters operating in the same frequency range. A novel procedure has been proposed that allows the design to be scaled up or down for other frequencies. A comparison between EM simulations and ideal model responses has shown reasonable agreement.

The proposed method is advantageous in modern multilayered microwave circuits such as microwave monolithic integrated circuits or low-temperature cofired ceramics technologies leading to compact filters with high selectivity and low insertion loss.

REFERENCES

1. G. Matthaei, L. Young, and E.M.T. Jones, *Microwave filters, impedance-matching networks, and coupling structures*, Artech House, Norwood, MA, 1980, Chapter 7, pp. 355–419.

2. D. Pozar, *Microwave engineering*, 3rd ed., Wiley, New York, 2005, pp. 412–416.
3. Z.D. Tan, J.S. Mandeep, S.I.S. Hassan, and M.F. Ain, Composite low pass filter design with T and π network on microstrip line, *Microwave J* 50 (2007), not available.
4. N. Arbabi, M. Najmabadi, M. Yagoub, and V. Devabhaktuni, A new SQP based space-mapping algorithm for on-chip spiral inductor optimization, *Proceeding of the Canadian Conference on Electrical and Computer Engineering (CCECE)*, Vancouver, Canada, 2007, pp. 99–102.
5. S. Pinel, R. Bairavasubramanian, J. Laskar, and J. Papapolymerou, Compact planar and vialess composite low-pass filters using folded stepped-impedance resonator on liquid-crystal-polymer substrate, *IEEE Trans Microwave Theory Tech* 53 (2005), 1707–1712.
6. S.N. Uysal, A compact coplanar stripline lowpass filter, *Proceedings of the Asia-Pacific Microwave Conference*, Singapore, 1999, pp. 307–310.
7. R.N. Martins and H. Abdalla, Design of low-pass microstrip filters with equal-ripple passband and finite attenuation poles, *Proceedings of the MTT-S International Microwave Optoelectronics Conference*, Belem, Brazil, 2001, pp. 71–74.
8. J. Zobel, Theory and design of uniform and composite electric wave filters, *Bell Syst Tech J* 2 (1923), 1–46.
9. J.-S. Hong, M.J. Lancaster, D. Jedamzik, and R.B. Greed, On the development of superconducting microstrip filters for mobile communications application, *IEEE Trans Microwave Theory Tech* 47 (1999), 1656–1663.
10. Agilent ADS, Available at: www.agilent.com/find/eesof-ads. Accessed on March 2011.
11. I.J. Bahl, *Lumped elements for RF and microwave circuits*, Artech House, Norwood, MA, 2003.
12. Micron Semiconductor Ltd., Available at: <http://www.micron-semiconductor.co.uk/product.asp>. Accessed on March 2011.
13. C.P. Yue, C. Ryu, J. Lau, T.H. Lee, and S.S. Wong, A physical model for planar spiral inductors on silicon, *Proceeding of the IEEE International Electron Devices Meeting Tech Digest*, San Francisco, CA, 1996, pp. 155–158.
14. Zeland IE3D, Available at: <http://www.mentor.com/electromagnetic-simulation/>. Accessed on February 2011.

BIOGRAPHIES



Navid Arbabi received the B.Sc. degree in Electrical Engineering (Electronics) from Ferdowsi University of Mashad, Iran, in 2005, and the M.A.Sc. degree in Electrical and Computer Engineering from Concordia University, Montreal, Canada, in 2008. He joined IDEA (Ajilon Consulting) in 2008, where he works as an IT consultant.



Mohammad Almalkawi received the Bachelor of Engineering degree in Telecommunications Engineering (with honors) from Yarmouk University, Irbid, Jordan, in 2007 and the M.Sc. degree in Electrical and Computer Engineering from South Dakota School of Mines and Technology, Rapid City, SD, USA, in 2009. He is currently working toward his Ph.D. at The University of Toledo, Toledo, USA. In the summer of 2011, he was an intern with Freescale Semiconductor, Inc., working on modeling RF/Microwave components for the development of product-level models. His current research interests include RF/Microwave circuit design and modeling, UWB antennas, and cross-talk reduction techniques in PCB interconnects.



Vijay Devabhaktuni received the B.Eng. degree in EEE and the M.Sc. degree in physics from BITS, Pilani, in 1996, and the Ph.D. in electronics from Carleton University, Canada, in 2003. He was awarded the Carleton University's senate medal at the Ph.D. level. During 2003–2004, he

held the Natural Sciences and Engineering Research Council (NSERC) postdoctoral fellowship and spent the tenure researching at the University of Calgary. In spring of 2005, he taught at Penn State Erie Behrend. During 2005–2008, he held the prestigious Canada Research Chair in Computer-Aided High-Frequency Modeling and Design at Concordia University, Montreal. Since 2008, he is an associate professor in the EECS Department at the University of Toledo. Dr. Devabhaktuni's R&D interests include applied electromagnetics, biomedical applications of wireless sensor networks, computer-aided design, device modeling, image processing, infrastructure monitoring, neural networks, optimization methods, RF/microwave devices, and virtual reality applications. In these areas, he secured external funding close to \$4M (sponsoring agencies include AFOSR, CFI, ODOT, NASA, NSERC, NSF, and industry). He coauthored 100 peer-reviewed papers, and is advising 17 M.S./Ph.D. students and three PDFs. He has won several teaching excellence awards in Canada and USA. Dr. Devabhaktuni currently serves as the Associate Editor of the *International Journal of RF and Microwave Computer-Aided Engineering*. He is a registered member of the Association of Professional Engineers, Geologists, and Geophysicists of Alberta and is a Senior Member of the IEEE.



Mustapha C.E. Yagoub received the Dipl.-Ing. degree in Electronics and the Magister degree in Telecommunications, both from the Ecole Nationale Polytechnique, Algiers, Algeria, in 1979 and 1987, respectively, and the Ph.D. degree from the Institut National Polytechnique, Toulouse, France, in 1994. After few years working in industry as a design engineer, he joined the Institute of

Electronics, Université des Sciences et de la Technologie Houari Boumédiène, Algiers, Algeria, first as an Lecturer during 1983–1991 and then as an Assistant Professor during 1994–1999. From 1996 to 1999, he has been head of the communication department. From 1999 to 2001, he was a visiting scholar with the Department of Electronics, Carleton University, Ottawa, ON, Canada, working on neural networks applications in microwave areas. In 2001, he joined the School of Information Technology and Engineering (SITE), University of Ottawa, Ottawa, ON, Canada, where he is currently a Professor. His research interests include RF/microwave CAD, RFID design, neural networks for high frequency applications, planar antennas, and applied electromagnetics. He has authored or coauthored over 300 publications in these topics in international journals and referred conferences. He authored *Conception de circuits linéaires et non linéaires micro-ondes* (Cépaduès, Toulouse, France, 2000), and coauthored *Computer Manipulation and Stock Price Trend Analysis* (Heilongjiang Education Press, Harbin, China, 2005). Dr. Yagoub is an Editorial Board member of the *International Journal of RF and Microwave Computer-Aided Engineering*, a senior member of the IEEE, and a registered member of the Professional Engineers of Ontario, Canada.



Arjuna Madanayake is an assistant professor at the Department of Electrical and Computer Engineering at the University of Akron in Ohio, USA. He completed the B.Sc. [Eng] Special Degree in Electronic and Telecommunication Engineering with First Class Honors from the University of Moratuwa, Sri Lanka, in 2001, followed by M.Sc. and Ph.D. degrees, both in Electrical Engineering, from the University of Calgary, Canada, in 2004 and 2008, respectively. Dr. Madanayake conducted postdoctoral research for the Institute of Space Imaging Science (ISIS) Canada during 2008–2009, where he investigated multidimensional signal processing algorithms and digital processors for Square Kilometer Array (SKA) systems as part of the Canadian SKA research effort. Dr. Madanayake was awarded the NSERC Postdoctoral Award and was nominated as the “Most outstanding candidate in Electrical Engineering and Computing Science” in the 2009 NSERC PDF Competition. His current research interests include multidimensional signal processing, digital VLSI/FPGA systems, SKA beamforming and RF antenna arrays, analog CMOS design for signal processing, and fast algorithms.